Journal of Visualized Experiments

Molecular Spring Constant Analysis by Biomembrane Force Probe Spectroscopy

--Manuscript Draft--

Article Type:	Invited Methods Collection - Author Produced Video
Manuscript Number:	JoVE62490R4
Full Title:	Molecular Spring Constant Analysis by Biomembrane Force Probe Spectroscopy
Corresponding Author:	Lining Arnold Ju, Ph.D. University of Sydney Darlington, NSW AUSTRALIA
Corresponding Author's Institution:	University of Sydney
Corresponding Author E-Mail:	arnold.ju@sydney.edu.au
Order of Authors:	Peyman Obeidy
	Haoqing Wang
	Mingqin Du
	Huiqian Hu
	Fang Zhou
	Haoruo Zhou
	Hao Huang
	Yunduo Charles Zhao
	Lining Arnold Ju, Ph.D.
Additional Information:	
Question	**Response**
Please indicate whether this article will be Standard Access or Open Access.	Standard Access (US$1200)
Please specify the section of the submitted manuscript.	Bioengineering
Please confirm that you have read and agree to the terms and conditions of the author license agreement that applies below:	I agree to the Author License Agreement
Please provide any comments to the journal here.	On behalf of all co-authors, I would like to thank Editor Dr. Kyle Jewhurst and Dr. Geetanjali Kamath, and Guest Editor Dr. Qian (Peter) Su for the invitation of this special edition.
Please indicate whether this article will be Standard Access or Open Access.	Standard Access ($1400)
Please confirm that you have read and agree to the terms and conditions of the video release that applies below:	I agree to the Video Release

Title:
Molecular Spring Constant Analysis by Biomembrane Force Probe Spectroscopy

Authors and Affiliations:
Peyman Obeidy[1], Haoqing Wang[1,2,3], Mingqin Du[1], Huiqian Hu[1,4], Fang Zhou[1], Haoruo Zhou[5], Hao Huang[5], Yunduo Charles Zhao[1,2], Lining Arnold Ju[1,2,3 †]

[1]*School of Biomedical Engineering, Faculty of Engineering, The University of Sydney, Darlington, NSW, Australia*
[2]*Charles Perkins Centre, The University of Sydney, Camperdown, NSW, Australia*
[3]*Heart Research Institute, Newtown, NSW, Australia*
[4]*Department of Chemistry, The Hong Kong University of Science and Technology, Clear Water Bay, Hong Kong, China*
[5]*School of Aerospace, Mechanical and Mechatronic Engineering, Faculty of Engineering, The University of Sydney, Darlington, NSW, Australia*

peyman.obeidy@sydney.edu.au
mingqin.du@sydney.edu.au
hhuaq@connect.ust.hk
fzho8451@uni.sydney.edu.au
jerry19961015@gmail.com
hzho5186@sydney.edu.au
hhua3090@uni.sydney.edu.au
yunduo.zhao@sydney.edu.au

[†]*Corresponding author:*
Lining Arnold Ju. Email: arnold.ju@sydney.edu.au

Keywords
Molecular spring constant, Biomembrane force probe, dynamic force spectroscopy, stretch assay, integrin.

Summary:
A biomembrane force probe (BFP) is an *in situ* dynamic force spectroscopy (DFS) technique. BFP can be used to measure the spring constant of molecular interactions on living cells. This protocol presents spring constant analysis for molecular bonds detected by BFP.

Abstract:
A biomembrane force probe (BFP) has recently emerged as a native-cell-surface or *in situ* dynamic force spectroscopy (DFS) nanotool that can measure single-molecular binding kinetics, assess mechanical properties of ligand–receptor interactions, visualize protein dynamic conformational changes and more excitingly elucidate receptor mediated cell mechanosensing mechanisms. More recently, BFP has been used to measure the spring constant of molecular bonds. This protocol describes the step-by-step procedure to perform molecular spring constant DFS analysis. Specifically, two BFP operation modes are discussed, namely the Bead–Cell and Bead–Bead modes. This protocol focuses on deriving spring constants of the molecular bond and cell from DFS raw data.

Introduction:
As a live-cell DFS technique, BFP engineers a human red blood cell (RBC; **Figure 1**) into an

ultrasensitive and tunable force transducer with a compatible spring constant range at 0.1-3 pN/nm[1,2,3]. To probe ligand–receptor interaction, BFP enables DFS measurements at ~1 pN (10^{-12} N), ~3 nm (10^{-9} m), and ~0.5 ms (10^{-3} s) in force, spatial, and temporal resolution[4,5]. Its experimental configuration consists of two opposing micropipettes, namely the probe and the target. The probe micropipette aspirates a RBC and a bead is glued at its apex via a biotin–streptavidin interaction. The bead is coated with the ligand of interest (**Figure 1A**). The target micropipette aspirates either a cell or a bead bearing the receptor of interest, corresponding to the Bead–Cell (**Figure 1B**) and Bead–Bead (**Figure 1C**) modes, respectively[5].

BFP construction, assembly and the DFS experimental protocols were described in detail previously[1,6]. Briefly, a BFP touch cycle consists of 5 stages: Approach, Impinge, Contact, Retract and Dissociate (**Figure 1D**). The horizontal RBC apex position is denoted as $\boldsymbol{x_{RBC}}$. At the beginning, the unstressed (zero-force) RBC deformation $\Delta\boldsymbol{x_{RBC}}$ is 0 (**Table 1**). The Target is then driven by a piezotranslator to impinge on and retract from the Probe bead (**Figure 1D**). The RBC probe is first compressed by the target with negative RBC deformation $\Delta\boldsymbol{x_{RBC}} < 0$. In the Bond event, the Retract stage transitions from a compressive to a tensile phase with positive RBC deformation $\Delta\boldsymbol{x_{RBC}} > 0$ (**Figure 2C and D**). According to Hooke's law, the BFP bearing force is able to be measured as $F = k_{RBC} \times \Delta\boldsymbol{x_{RBC}}$, where k_{RBC} (**Table 1**) is the RBC spring constant of the BFP. Upon bond rupture and the completion of one touch cycle, the probe bead returns to zero-force position with $\Delta\boldsymbol{x_{RBC}} = 0$ (**Figure 1D**).

To determine the k_{RBC}, we measure and record the radii of the probe micropipette inner orifice (R_p), the RBC (R_0) and the circular contact area (R_c) between the RBC and the probe bead (**Figure 1A**). Then k_{RBC} is calculated according to the Evan's model (Eq. 1)[7,8] using a LabVIEW program that acts as a virtual instrument (VI) to operate the BFP (**Figure S1A**)[8,9].

$$\boldsymbol{k_{RBC}} = \frac{\pi \boldsymbol{R_p} \Delta \boldsymbol{p}}{(\mathbf{1}-\frac{\boldsymbol{R_p}}{\boldsymbol{R_0}})\boldsymbol{ln}\,(\frac{4{\boldsymbol{R_0}}^2}{\boldsymbol{R_p R_c}})} \quad \text{(Eq. 1)}$$

With a BFP established and DFS raw data obtained, hereby we present how to analyze the spring constant of ligand–receptor pair or cells. The DFS raw data on the interaction of the glycosylated protein Thy-1 and K562 cell bearing integrin $\alpha_5\beta_1$ (Thy-1–$\alpha_5\beta_1$; **Figures 3A** and **3B**)[10] and that of the fibrinogen and bead coated integrin $\alpha_{IIb}\beta_3$ (FGN–$\alpha_{IIb}\beta_3$; **Figure 3C**)[11,12] have been used to demonstrate the Bead–Cell and Bead–Bead analysis modes, respectively.

BFP Experimental Preparation

For details of BFP experimental preparation and instrumentation, please refer to the previously published protocols[3]. In brief, human RBC has been biotinylated using the Biotin–PEG3500–NHS in the carbon/bicarbonate buffer. Proteins of interest have been covalently coupled to the borosilicate glass beads using MAL–PEG3500–NHS in the phosphate buffer. To attach to the biotinylated RBC, the probe bead is also coated with streptavidin (SA) using the MAL–SA. Please see the **Table of Materials** and **Table 2**.

To assemble the BFP (**Figure 1**, *left*), the third micropipette termed 'Helper' will be used to deliver the probe bead and glue it to the RBC's apex[1,3]. The covalent interaction between the SA coated probe bead and biotinylated RBC is much stronger than the ligand–receptor bond of interest. Thus, the Dissociate stage can be interpreted as the ligand–receptor bond rupture rather than the detachment of Probe bead from the RBC.

Protocol:

1. Obtain Analyzable DFS Events

1.1. Start the experiment in the software (e.g., LabVIEW VI) for the BFP control and parameter setting (**Figure S1A**).

1.2. Observe the repetitive probe bead–target bead/cell touches in the software for BFP Monitor (**Figure S1B**).

1.3. Test and achieve the adhesion frequency ≤ 20% within the first 50 touches by tuning the impingement force and contact time, by which it ensures that ≥ 89% of DFS adhesion event are mediated by single bonds[12-14].

NOTE: For each Bead–Cell/Bead pair, we perform 200 repetitive touch cycles. To obtain publishable data quality, we usually perform n ≥ 3 Bead–Bead or Bead–Cell pairs.

1.3.1. Save data, in the form of Force vs. Time, to the user directed folder by the end of each pair, prompted by the software for BFP control and parameter setting.

1.4. Collect the Force vs. Time raw data of Bond events, as exemplified in the **Figure 2A**, using the BFP acquisition platform (**Figure S1C**).

1.4.1. Open the BFP data analysis software. Click on the yellow folder icon and select the corresponding raw data file by double clicking on them.

1.5. Run the program, and then click the up and down button to switch between events. Use the outlier exclusion criteria (**Figure S2**) to screen out invalid events. Select the exporting data type as Force vs. Time format and click on the **Export Plots Data** button.

2. Convert the Force vs. Time Curve to the Force vs. Displacement Curve

2.1. Export the data segment corresponding to the Retract stage to a spreadsheet (**Figure 2A**, *square marquee*), which is relevant to the spring constant analysis.

2.2. Plot the Force vs. Time Curve using spreadsheet software. To obtain the Force vs. Displacment curve, convert the time values (**Figure 2A**, *x*-axis) to the total displacement values ($\Delta \boldsymbol{x}_{\mathbf{tot}}$) by multiplying time values with piezo movement velocity (i.e., 4,000 nm/s by preset).

2.3. Zero the first data point by subtracting the smallest displacement value from each acquired displacement value. This horizontal transformation does not affect the ascending slopes of the Retract stage nor the subsequent spring constant calculation.

2.4. Notably, the BFP is considered as a serial spring system in which $\Delta \boldsymbol{x}_{\mathbf{tot}}$ (**Table 1**) sum deformations of the RBC, $\Delta \boldsymbol{x}_{\mathbf{RBC}}$ (**Table 1**), the molecular bond, $\Delta \boldsymbol{x}_{\mathbf{mol}}$ (**Table 1**), and the Target cell, $\Delta \boldsymbol{x}_{\mathbf{cell}}$ (**Table 1**), as the Eq. 2:

$$\Delta \boldsymbol{x}_{\mathbf{tot}} = \Delta \boldsymbol{x}_{\mathbf{RBC}} + \Delta \boldsymbol{x}_{\mathbf{mol}} + \Delta \boldsymbol{x}_{\mathbf{cell}} \quad \text{(Eq. 2)}$$

2.5. Plot the Force (F) vs. Displacement ($\Delta \boldsymbol{x}_{\mathbf{tot}}$) curve as shown in the **Figure 2B**.

3. Spring Cnstant Analysis of Bead–Cell Mode

3.1. In the Force vs. Displacement curve, two distinct slop can be identified, where each can represent the compressive phase and the tensile phase. Fit a regression line to each data group (**Figure 2B**), where the larger linear fit slope represents the total spring constant at compressive phase (**Figure 2B**, *red*), denoted as k_1 (**Table 1**); and the smaller linear fit slope represents the total spring constant at tenslile phase (**Figure 2B**, *blue*), denotated as k_2 (**Table 1**).

3.2. For springs connected in series per step 2.2 description, express the reciprocal of the total spring constant, k_{tot} (**Table 1**), as the sum of the spring constant inverses of RBC, k_{RBC} (**Table 1**), the molecular bond, k_{mol} (**Table 1**), and the Target cell, k_{cell} (**Table 1**). During the compressive phase of the Bead–Cell mode, the molecular bond is not stretched, therefore k_{mol} is not taken into consideration. The reciprocal of the k_{tot} in this scenario ($1/k_1$) is expressed as

$$\frac{1}{k_1} = \frac{1}{k_{RBC}} + \frac{1}{k_{cell}} \text{ (Eq. 3).}$$

In the example data, k_{RBC} is pre-determined (0.25 pN/nm by default). k_{cell} can be derived from the Eq. 3 with the acquired k_1 and k_{RBC} (**Figure 3B**).

3.3. During the tensile phase, adhesion is formed between the ligand–receptor pair. Express the reciprocal of the k_{tot} in this scenario ($1/k_2$) as

$$\frac{1}{k_2} = \frac{1}{k_{RBC}} + \frac{1}{k_{mol}} + \frac{1}{k_{cell}} \text{ (Eq. 4)}$$

where k_2 (**Table 1**) represents the total spring constant during the tensile phase.

3.4. Derive k_{mol} from subtracting $1/k_1$ from $1/k_2$ (compare Eq. 3 vs. Eq. 4).

4. Spring Constant Analysis of Bead–Bead Mode

4.1. Fit a regression line to the compressive phase data to obtain k_1 (similar to the **Figure 2B**, *red*). Of note, in the Bead–Bead mode, the Target cell is replaced by a glass bead coated with the receptor of interest (**Figure 1C**). Since bead deformation is negligible, the $1/k_{cell}$ term can be removed from the Eq. 3 and Eq. 4 accordingly. The reciprocal k_{tot} of the compressive phase ($1/k_1$) can be expressed as:

$$\frac{1}{k_1} = \frac{1}{k_{RBC}} \text{ (Eq. 5)}$$

4.2. Fit a regression line to the tensile phase data to obtain k_2 (similar to the **Figure 2B**, *blue*). The reciprocal k_{tot} of the tensile phase ($1/k_2$) can be expressed as:

$$\frac{1}{k_2} = \frac{1}{k_{RBC}} + \frac{1}{k_{mol}} \text{ (Eq. 6)}$$

4.3. Derive k_{mol} from subtracting $1/k_1$ from $1/k_2$ (compare Eq. 5 vs. Eq. 6).

Representative Results:

In this work, we have demonstrated the protocol of the BFP spring constant analysis. For the Bead–Cell analysis mode, we analyzed the k_{mol} of the molecular bond between the glycosylated protein Thy-1 coated on the Probe bead and the integrin $\alpha_5\beta_1$ expressed on the Target K562 cell (Thy-1–integrin $\alpha_5\beta_1$; **Figure 3A**)[10]. The k_{cell} is also derived from the Bead–Cell mode (K562 Cell; **Figure 3B**). For the Bead–Bead mode, the molecular bond formed between fibrinogen and integrin $\alpha_{IIb}\beta_3$ (FGN–integrin $\alpha_{IIb}\beta_3$; **Figure 3C**)[11,12] is used to demonstrate the Bead–Bead analysis mode.

For the Bead–Cell mode, we measured the spring constants of Thy-1–integrin $\alpha_5\beta_1$ bond and K562 cell as k_{mol} = 0.45 ± 0.28 pN/nm (**Figure 3A**) and k_{cell} = 0.18 ± 0.07 pN/nm (**Figure 3B**) from 27 pre-screened analyzable events. For the Bead–Bead mode, we measured the spring constants of FGN–integrin $\alpha_{IIb}\beta_3$ bond as k_{mol} = 0.53 ± 0.29 pN/nm (**Figure 3C**) from 33 pre-screened analyzable events.

Table 1. Symbol definitions for the BFP molecular spring constant analysis. Horizontal positions of all objects are defined as $\boldsymbol{x}$, while $\Delta\boldsymbol{x}$ [nm] refers to the deformation relative to the original position. ΔF [pN] refers to the force increment measured by BFP. k [pN/nm] refers to the spring constant. Subscripts 1 and 2 correspond to the compressive and tensile phases, respectively. The molecular spring constant is derived from the Force (F) vs. Displacement (Δx_{tot}) curve.

Figure 1: BFP configuration and DFS touch cycle. (A) The BFP system assembles two opposing micropipettes, namely the Probe (*left*) and the Target (*right*). The Probe micropipette aspirates a RBC (*red*) with a glass bead glued at its apex to serve as a force transducer. The Target micropipette aspirates a receptor-bearing cell (*blue*). The RBC spring constant (k_{RBC}) is determined by the aspiration pressure (Δp) and the radii of aspirated RBC (R_0), Probe micropipette (R_p) and circular contact area (R_c) between the RBC and the Probe bead. **(B and C)** Micrographs of the Bead–Cell (B) and Bead–Bead (C) BFP modes. Scale bars = 5 μm. **(D)** A BFP touch cycle that consists of Approach, Impinge, Contact, Retract and Dissociate stages. The $\Delta\boldsymbol{x}_{\mathbf{RBC}}$ = 0 dash line indicates the BFP unstressed, or zero-force, position. The Retract stage includes compressive phase ($\Delta\boldsymbol{x}_{\mathbf{RBC}} < 0$, *red*), zero-force position ($\Delta\boldsymbol{x}_{\mathbf{RBC}} = 0$, *black*) and tensile phase ($\Delta\boldsymbol{x}_{\mathbf{RBC}} > 0$, *blue*) in sequence. Black arrow indicates the position of Bond event.

Figure 2: Derive molecular spring constants from DFS raw data. (**A**) Representative Force (F) vs. Time (t) curve of DFS raw data in one BFP touch cycle. (**B**) Representative converted Force (F) vs. Displacement ($\Delta\boldsymbol{x}_{\mathbf{tot}}$) curve that depicts the Retract stage. k_1 and k_2 represent the fit slope of the consecutive compressive and tensile phases respectively. ΔF_1 and ΔF_2 represent the increments of force in the compressive phase and the tensile phase data, respectively, where $\Delta\boldsymbol{x}_1$ and $\Delta\boldsymbol{x}_2$ represent the increments of displacement in the compressive phase and tensile phase data, respectively. R^2 values for spring constant during compressive stage (R_1^2) and tensile phase (R_2^2) are labelled on the graph to indicate good statistical fitness. (**C and D**) Illustrations of the Retract stage in the Bead–Cell (C) and Bead–Bead (D) experimental modes. k_{RBC} represents the spring constant of RBC; k_{cell} and k_{mol} represent the spring constants of the Target cell and the molecular bond, respectively. During the tensile phase, adhesion is formed between the ligand–receptor pair, the RBC deflects in the same direction as piezo retracts beyond zero-force position ($\Delta\boldsymbol{x}_{\mathbf{RBC}} > 0$).

Figure 3: Representative histograms of BFP measured spring constants. The event number (*left y-axis*) and frequency distribution (*right y-axis*) of measured spring constants for Thy-1–integrin $\alpha_5\beta_1$ bond (A) and K562 Target cell (B) in the Bead–Cell mode and FGN–integrin $\alpha_{IIb}\beta_3$ bond (C) in the Bead–Bead mode. Histograms are fit with Gaussian distribution curve (*pink*) and the statistical parameter, R^2, is used to indicate the strength of fitness.

Figure S1: The homemade BFP interface. (**Ab** BFP control and parameter setting interface. The parameters to determine RBC spring constant are entered from the panel of biophysical parameters. **(B)** BFP monitoring. Live BFP touch cycles will be observed from this camera view. **(C)** BFP DFS analysis interface where the Force (F) vs. Time (t) curves are offline reviewed and pre-processed for subsequent molecular spring constant analysis.

Figure S2. BFP analyzable data quality control and pre-screening criteria. (**A**) Good DFS events with high quality: (i) Bead–Cell rupture force event; (ii) Bead–Cell lifetime event; (iii) Bead–Bead rupture force event; (iv) Bead–Bead lifetime event. (**B**) Acceptable DFS events with some noise: (i) Data drifting but the zoom-in Retract stage remains valid; (ii)Slight data drifting after bond dissociation; (iii) Data kink at the zero-force regime; (iv) Holding force is small (< 10 pN). (**C**) Poor-quality events that should be discarded: (i) No adhesion; (ii) Data oscillation; (iii) Data drifting all the time; (iv) Discontinuous data; (v) Compressive force too small (≈ 0 pN); (vi) Multiple bonds; (vii) Invalid data with derived $k_{mol} < 0$; (viii) Signal error. Zero force is indicated by the grey intermittent line.

Discussion:

In summary, we have provided a detailed data analysis protocol for preprocessing the DFS raw data and deriving molecular spring constants in the BFP Bead–Bead and Bead–Cell analysis modes. Biomechanical models and equations required for determining molecular and cellular spring constants are presented. Albeit different integrins are studied, the k_{mol} measured by the Bead–Bead mode and the Bead–Cell mode possesses significant range differences (**Figure 3A** vs. **Figure 3C**). Of note, with the Bead–Bead mode, the receptor is covalently linked to the glass bead. In contrast, with the Bead–Cell mode, the surface receptor is adapted by the underlying plasma membrane and cytoskeletons, which most likely influence the measured k_{mol}.

Data quality control is crucial to ensure the reproducibility. To this end, we have implemented the DFS data pre-screening and outlier exclusion criteria on the Force vs. Time plots. To demonstrate this, a representative dataset was selected, in which we categorized the DFS raw data into three levels of quality: Good (**Figure S2A**), Acceptable with noise (**Figure S2B**), and Poor unacceptable (**Figure S2C**). For beginners of using the BFP, we recommend the strict criteria to pre-screen the data with the Good quality (**Figure S2A**). Of note, based on the data pre-screening criteria, the regression fit line of the compressive phase should be steeper than that of the tensile phase, specifically $k_1 > k_2$ (**Figure S2C**, vii). When measured $k_1 < k_2$ (**Figure S2C**, vii), the derived $k_{mol} < 0$ is against the rationale per calculation in the step 4. Such events should then be considered as the invalid outliers and discarded.

To favor the BFP measurement on single-molecular level during data acquisition, multiple experimental configurations have been implemented according to previous study[12]. Firstly, protein coating density on beads is usually titrated down to a minimal level (e.g. 60 μm^{-2}) by strictly control the solution concentration, quantity of the protein and reaction conditions[15]. The average spatial distance between proteins on the bead is thereby estimated much larger than the linear dimensions of the protein, favoring our measurements on single-molecular level[12-14]. Secondly, we control the adhesion frequency for each ligand–receptor pair ≤ 20%, under which molecular binding events will follow Poisson distribution predicting ≥ 89% of events would be single-molecular binding[14,15]. To achieve so, impingement force and contact time are set accordingly and need to be consistent throughout the experiment[12]. Nevertheless, it is still possible that multiple bonds occur sequentially (**Figure S2C**, vi). In such cases, we will discard the events with signatures of multiple bonds. Last but not least, negative control experiments will be performed with beads coated with bovine serum albumin (**Table of Materials**) or SA alone to ensure the non-specific adhesion frequency is ≤ 2%[16,17].

Although BFP is powerful to investigate protein dynamics on living cell surface[10-12], there are technical limitations. In BFP, only one ligand–receptor pair can be investigated at a time. It

would be time consuming to obtain sufficient data with statistical significance. Besides, the experimental procedures are labor intensive with steep learning curves. Implementation wise, the current BFP system is susceptible to the environmental drifting and surrounding mechanical vibration. As a result, continuous manual adjustment is required to ensure the DFS data quality. To this end, one of our recent studies has introduced ultra-stable BFP feedback control algorithms to improve the stability of the BFP force-clamp DFS assays[4]. This technical advance enables measurements of stronger molecular interaction such as antigen–antibody binding with ultra-long bond lifetime (>50 s). Nevertheless, we foresee future efforts will be made to automate and integrate the BFP data acquisition and DFS analysis into one computerized program, making the entire BFP operation and data analysis more user friendly and high-throughput.

Acknowledgements:
We thank Guillaume Troadec for helpful discussion, Zihao Wang for hardware consultation, and Sydney Manufacturing Hub, Gregg Suaning and Simon Ringer for support of our lab startup. This work was supported by Australian Research Council Discovery Project (DP200101970 - L.A.J.), NSW Cardiovascular Capacity Building Program (Early-Mid Career Researcher Grant - L.A.J.), Sydney Research Accelerator prize (SOAR - L.A.J.), Ramaciotti Foundations Health Investment Grant (2020HIG76 - L.A.J.), National Health and Medical Research Council Ideas Grant (APP2003904 - L.A.J.), and The University of Sydney Faculty of Engineering Startup Fund and Major Equipment Scheme (L.A.J.). Lining Arnold Ju is an Australian Research Council DECRA fellow (DE190100609).

Disclosures:
The authors declare that they have no competing interests to report regarding the present study.

References:
1 Chen, Y. *et al.* Fluorescence Biomembrane Force Probe: Concurrent Quantitation of Receptor-ligand Kinetics and Binding-induced Intracellular Signaling on a Single Cell. *The Journal of Visualized Experiments.* 10.3791/52975 (102), e52975 (2015).
2 Su, Q. P., Ju, L. A. Biophysical nanotools for single-molecule dynamics. *Biophysics Reviews.* **10** (5), 1349-1357 (2018).
3 Ju, L. Dynamic Force Spectroscopy Analysis on the Redox States of Protein Disulphide Bonds. *Methods in Molecular Biology.* **1967**, 115-131 (2019).
4 An, C. *et al.* Ultra-stable Biomembrane Force Probe for Accurately Determining Slow Dissociation Kinetics of PD-1 Blockade Antibodies on Single Living Cells. *Nano Letters.* **20** (7), 5133-5140 (2020).
5 Chen, Y., Ju, L., Rushdi, M., Ge, C., Zhu, C. Receptor-mediated cell mechanosensing. *Molecular Biology of the Cell.* **28** (23), 3134-3155 (2017).
6 Ju, L., Chen, Y., Rushdi, M. N., Chen, W., Zhu, C. Two-Dimensional Analysis of Cross-Junctional Molecular Interaction by Force Probes. *Methods in Molecular Biology.* **1584**, 231-258 (2017).
7 Evans, E., Ritchie, K., Merkel, R. Sensitive force technique to probe molecular adhesion and structural linkages at biological interfaces. *Biophysical Journal.* **68** (6), 2580-2587 (1995).
8 Ju, L., Zhu, C. Benchmarks of Biomembrane Force Probe Spring Constant Models. *Biophysical Journal.* **113** (12), 2842-2845 (2017).
9 Evans, E., Ritchie, K, Merkel, R. Sensitive Force Technique to Probe Molecular Adhesion and Structural Linkages at Biological Interfaces. *Biophysical Journal.* **68**, 2580-1587 (1995).

10 Fiore, V. F., Ju, L., Chen, Y., Zhu, C., Barker, T. H. Dynamic catch of a Thy-1-alpha5beta1+syndecan-4 trimolecular complex. *Nature Communications.* **5**, 4886 (2014).
11 Passam, F. *et al.* Mechano-redox control of integrin de-adhesion. *Elife.* **7** (2018).
12 Chen, Y. *et al.* An integrin alphaIIbbeta3 intermediate affinity state mediates biomechanical platelet aggregation. *Nature Materials.* **18** (7), 760-769 (2019).
13 Chen, Y., Lee, H., Tong, H., Schwartz, M., Zhu, C. Force regulated conformational change of integrin αVβ3. *Matrix Biology.* **60**, 70-85 (2017).
14 Liu, B., Chen, W., Zhu, C. Molecular force spectroscopy on cells. *Annual Review of Physical Chemistry.* **66**, 427-451 (2015).
15 Piper, J. W., Swerlick, R. A., Zhu, C. Determining force dependence of two-dimensional receptor-ligand binding affinity by centrifugation. *Biophysical Journal.* **74** (1), 492-513 (1998).
16 Ju, L., Dong, J.-f., Cruz, M. A., Zhu, C. The N-terminal flanking region of the A1 domain regulates the force-dependent binding of von Willebrand factor to platelet glycoprotein Ibα. *Journal of Biological Chemistry.* **288** (45), 32289-32301 (2013).
17 Ju, L., Chen, Y., Xue, L., Du, X., Zhu, C. Cooperative unfolding of distinctive mechanoreceptor domains transduces force into signals. *Elife.* **5**, e15447 (2016).

Figure 1

Click here to access/download;Figure;Fig 1.tif

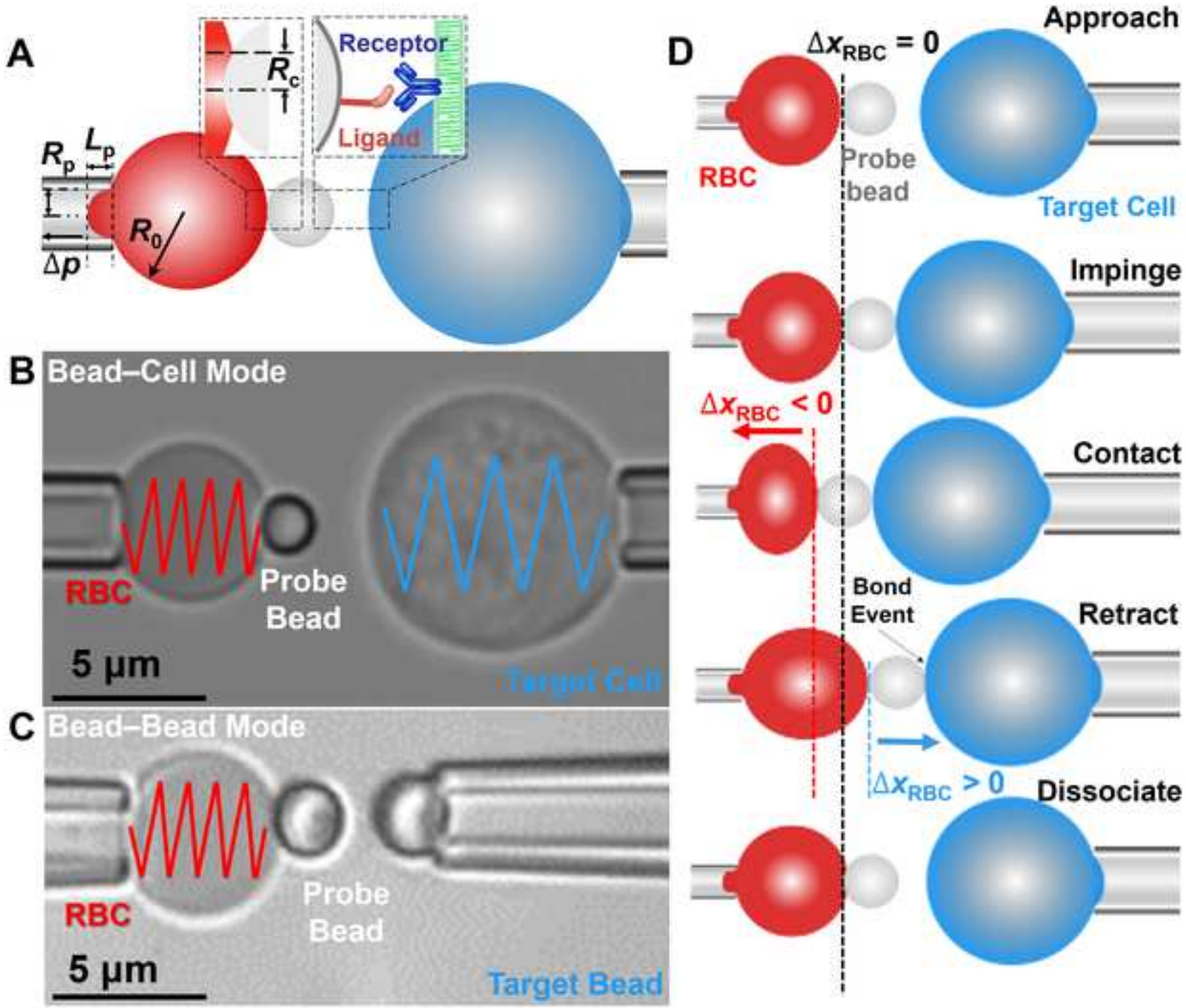

Figure 2

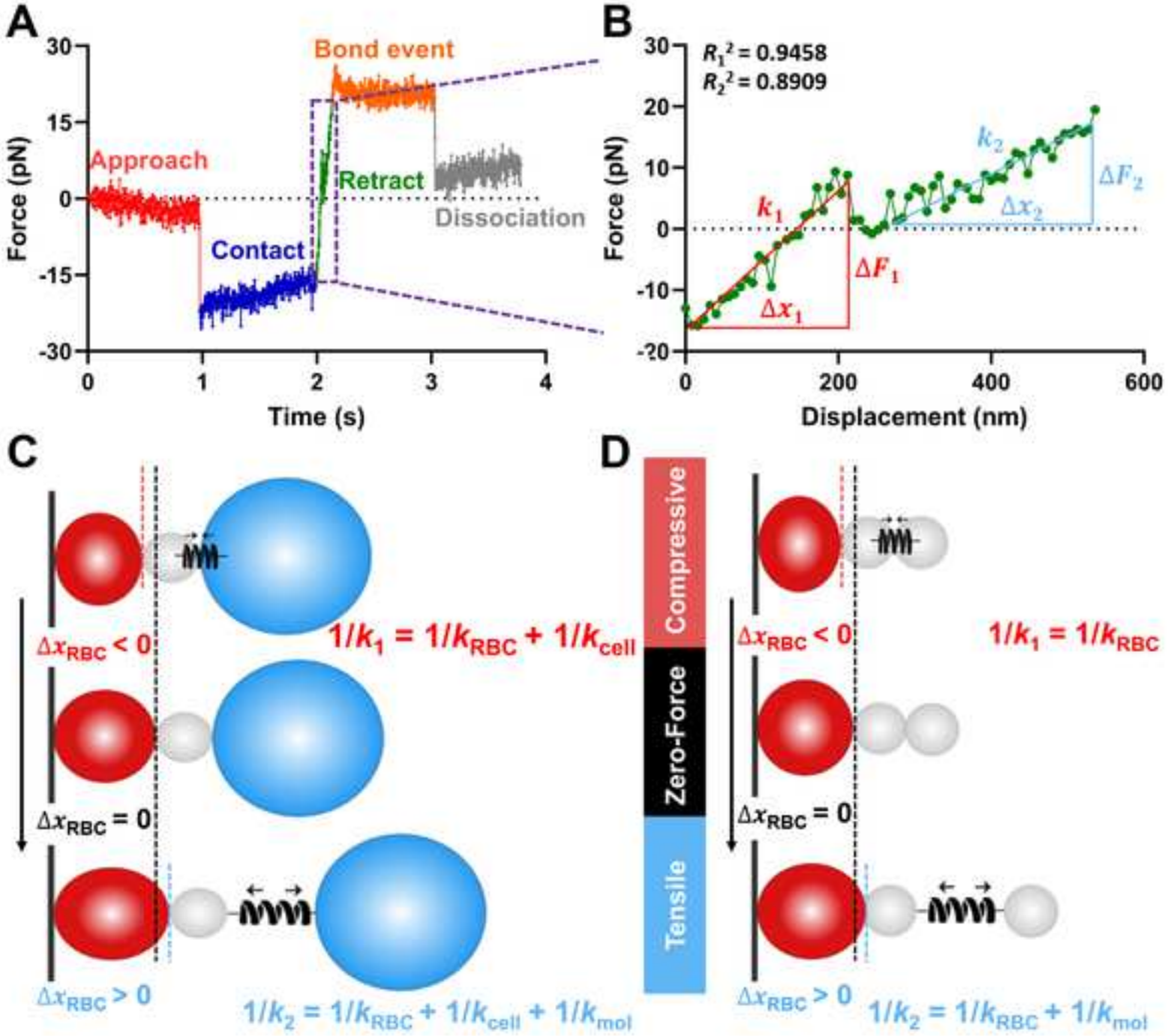

Figure 3

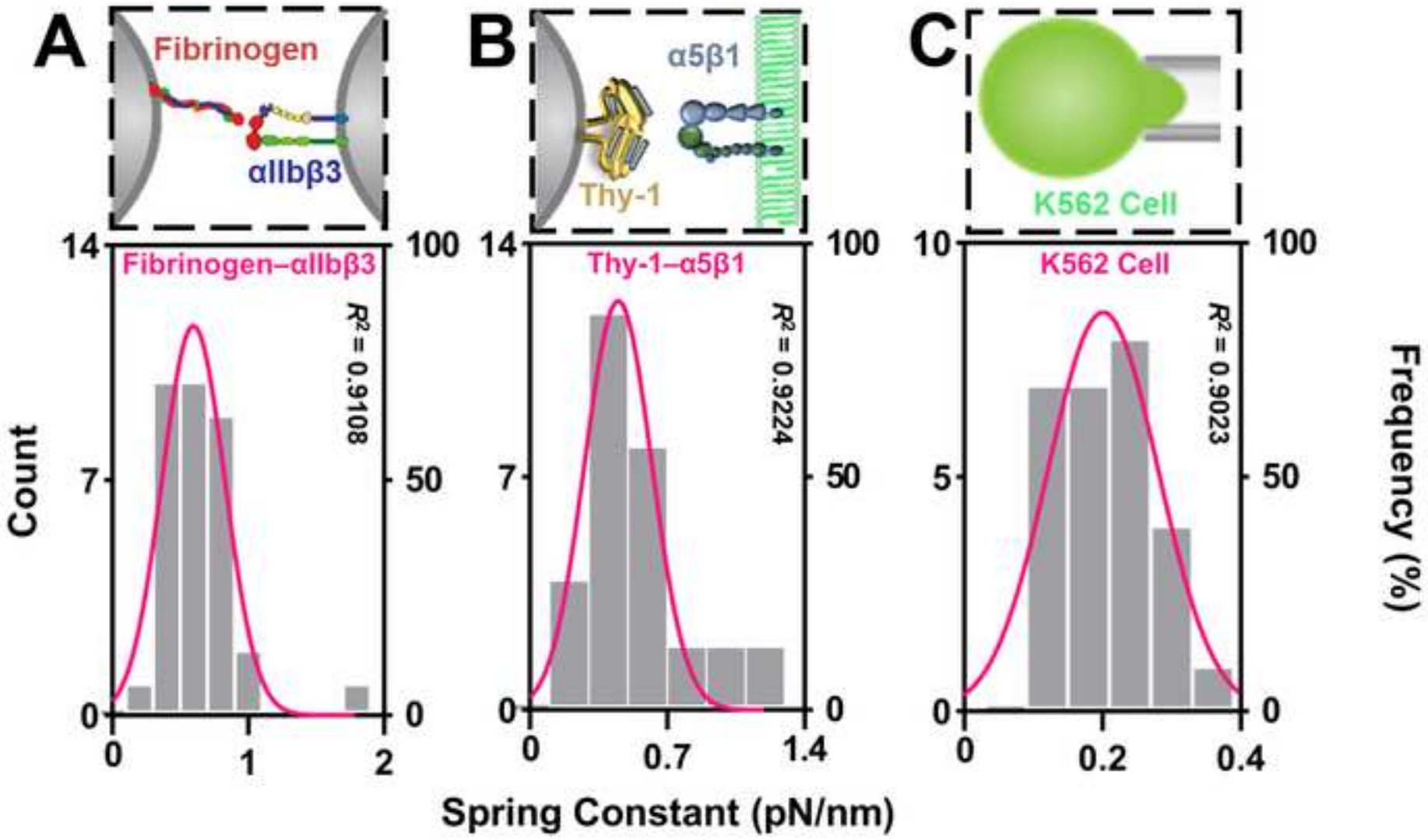

Table 1: Main DFS Parameters for BFP spring constant analysis.

Symbol	Definition	Symbol	Definition
Δx_{tot}	The total displacement of the piezo, which can also be interpreted as the total deformation of RBC, target cell and molecular bond.	Δx_{RBC}	The RBC deformation, which can also be interpreted as the displacement of the Probe bead.
k_{tot}	The total spring constant of the entire BFP serial spring system.	k_{RBC}	The spring constant of the aspirated RBC by the Probe micropipette.
k_{mol}	The spring constant of the BFP detected molecular bond	k_{cell}	The spring constant of the Target cell.
k_1	k_{tot} of the compressive phase in the Retract stage.	k_2	k_{tot} of the tensile phase in the Retract stage.
ΔF_1	The increment of force sensed by the Probe bead in the compressive phase.	ΔF_2	The increment of force sensed by the Probe bead in the tensile phase.
Δx_1	The increment of displacement in the compressive phase.	Δx_2	The increment of displacement in the tensile phase.

Carbonate/bicarbonate buffer (pH 8.5)	
Sodium Carbonate (Na_2CO_3)	8.4 g/L
Sodium Bicarbonate ($NaHCO_3$)	10.6 g/L
Phosphate buffer (pH 6.5-6.8)	
NaPhosphate monobasic $NaH_2PO_4 \bullet H_2O$	27.6 g/L
Anhy. NaPhosphate dibasic Na_2HPO_4	28.4 g/L
10× Tyrode's buffer	
$NaHCO_3$	120 mM
HEPES	100 mM
NaCl	1.37 M
KCl	27 mM
D-glucose	55 mM

Click here to access/download

Table of Materials

Materials.xlsx

THE UNIVERSITY OF SYDNEY

SCHOOL OF BIOMEDICAL ENGINEERING

FACULTY OF ENGINEERING

arnold.ju@sydney.edu.au
School of Biomedical Engineering
The University of Sydney
Blackwattle Creek Ln, Darlington,
NSW, AUSTRALIA 2008

Camperdown, NSW, AUSTRALIA 2006

August 20th, 2021

Dr Nam Nguyen

Manager of Review, JoVE

Dear Dr Geetanjali Kamath:

On behalf of all co-authors, I would like to express my sincerely thank for your favorable and meticulous support with comments on our manuscript entitled with “Molecular Spring Constant Analysis by Biomembrane Force Probe Spectroscopy”. We also wish to thank the invitation from Editor Dr. Kyle Jewhurst and Guest Editor Dr. Qian (Peter) Su for this special edition in Biophysical nanotools for molecular dynamics at nanoscale, Methods Collections. We have thoroughly addressed all comments point-by-point in the response and the revised manuscript.

We have great appreciation for the Editorial and Production Comments. Hereby, we followed the editor’s original guideline and comments for both video and manuscript with the following changes in the point-by-point format with blue response and actions taken.

Changes to be made by the Author(s) regarding the written manuscript:
1. Please increase the homogeneity between the written protocol and the video narration. Please watch the video while reading the written protocol. Uniting the language between both would greatly allow users to follow along. Please see the comments in the attached manuscript.
We modify the written protocol to unite the language between manuscript and video narration.

Changes to be made by the Author(s) regarding the video:
1. Title Card:
• Please capitalize on the first letter of every important word in your every chapter title cards.
First letters of every important word in all chapter title cards are capitalized.

• Please maintain the same style in every chapter title cards.
We revised the chapter title cards to ensure consistency of style.

2. Audio Editing and Pacing:
00:46 - 02:02 The audio seems to be garbled and over-processed, as though a noise reduction filter has been applied. Consider reprocessing the audio with a weaker setting.
We revised the soundtrack to fix the problem of garbled and over-processed.

We are grateful for your consideration and look forward to acceptance of this work from you at the earliest convenience.

Sincerely,

Arnold Lining Ju, PhD (Georgia Tech & Emory)
Assistant Professor of Biomedical Engineering (Senior Lecturer)
Australian Research Council DECRA Fellow
National Heart Foundation Paul Korner Future Leader Fellow

Address The University of Sydney, Faculty of Engineering, School of Biomedical Engineering
Room S407, Mechanical Engineering Building (J07), Blackwattle Creek Ln, Darlington, NSW 2008
T +61 2 9351 7140 | **E** arnold.ju@sydney.edu.au
W https://sydney.edu.au/engineering/about/our-people/acz ademic-staff/arnold-ju.html

Supplemental figure 1

Click here to access/download;Supplemental File (Figures, Permissions, etc.);Fig S1.tif

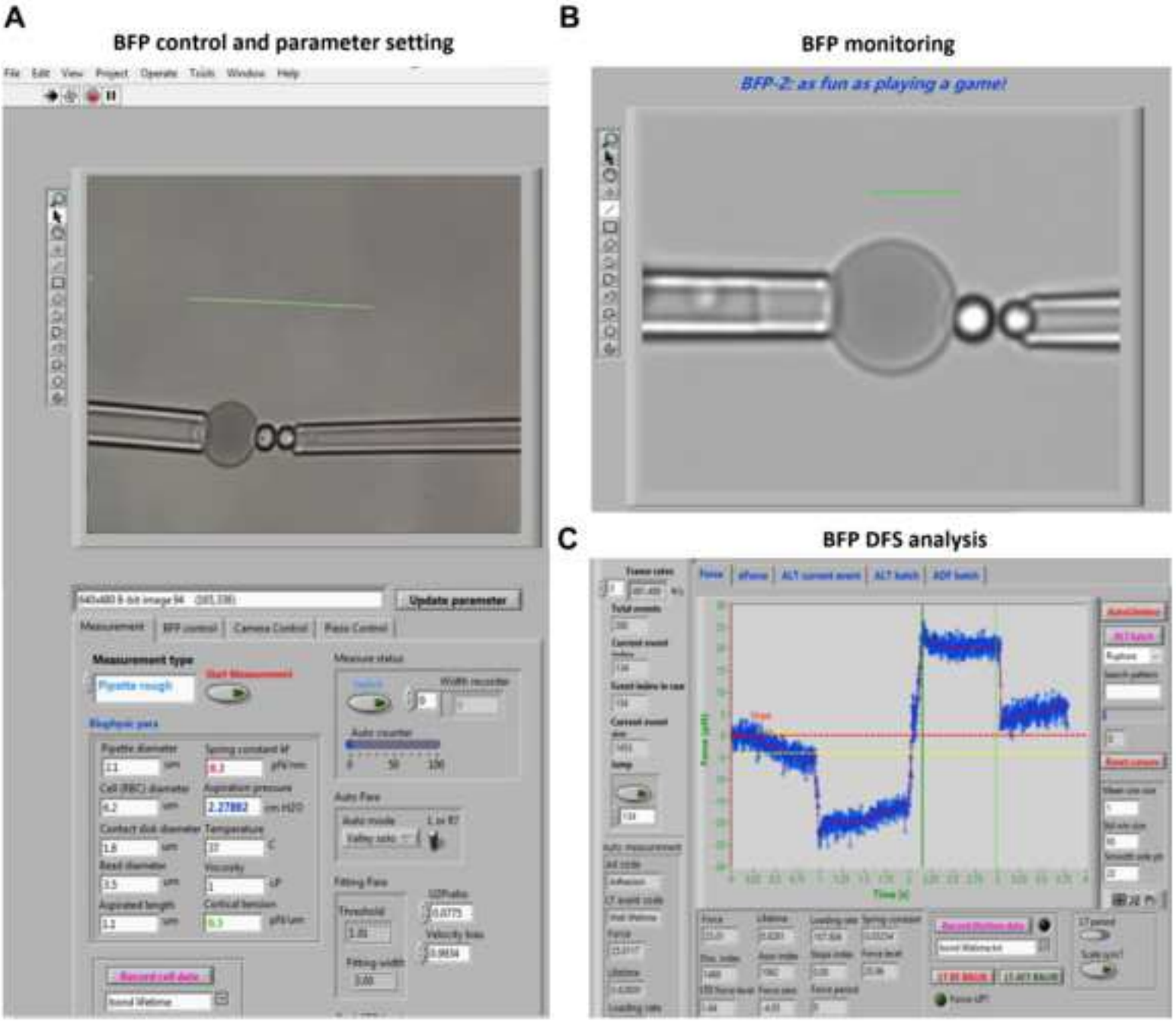

Supplemental figure 2

Click here to access/download;Supplemental File (Figures, Permissions, etc.);Fig S2.tif